Zosteric acid and salicylic acid bound to a low density polyethylene surface successfully control bacterial biofilm formation

C. Cattò[a,b], G. James[b], F. Villa[a], S. Villa[c], F. Cappitelli[a]*

[a]*Department of Food Environmental and Nutritional Sciences, Università degli Studi di Milano, Milano, Italy;* [b]*Center for Biofilm Engineering, Montana State University, Bozeman, MT, USA;* [c]*Department of Pharmaceutical Sciences, Università degli Studi di Milano, Milano, Italy.*

*Corresponding author: E-mail: francesca.cappitelli@unimi.it.

Abstract

The active moieties of the anti-biofilm natural compounds zosteric (ZA) and salicylic (SA) acids have been covalently immobilised on a low density polyethylene surface (LDPE). The grafting procedure provided new non-toxic eco-friendly materials (LDPE-CA and LDPE-SA) with anti-biofilm properties superior to the conventional biocide-based approaches and with features suitable for applications in challenging fields where the use of antimicrobial agents is limited. Microbiological investigation proved that LDPE-CA and LDPE-SA: i) reduced *Escherichia coli* biofilm biomass up to the 61% with a mechanism that did not affect bacterial viability; ii) significantly affected biofilm morphology decreasing biofilm thickness, roughness, substratum coverage, cell and matrix polysaccharide bio-volumes by more than 80% and increasing the surface to bio-volume ratio; iii) made biofilm more susceptible toward ampicillin and ethanol. Since no molecules were leached from the surface, they remained constantly effective and below the lethal level; therefore, the risk of developing resistant strains was minimised.

Keywords: zosteric acid, salicylic acid, anti-biofilm, bio-hybrid material, surface functionalization

Introduction

The main strategy for preventing biofilm-mediated damages in medical and industrial settings relies on routine cleaning and disinfection of microbial contact surfaces (Simões et al. 2010). Unfortunately, these approaches are not universally effective because sessile microorganisms display increased tolerance to conventional antimicrobial agents (Hall-Stoodley et al. 2004). In addition, resistance towards many antibiotics has emerged in many pathogenic microbial taxa (Sousa et al. 2014; Ventola 2015).

The modification of the surface properties by incorporating disinfectants, antiseptics, antibiotics and metallic nanoparticles into polymeric materials has been proposed as a promising strategy to tackle the current challenge in controlling biofilm growth (Coenye et al. 2011; Chen et al. 2013; Lo et al. 2014; Ahire et al. 2016). However, despite some of these materials are commercially available and already used in several applications, their real efficacy and recurrent drawbacks have made their use questionable (Chen et al. 2013; Pechook et al. 2015). Most of biocidal-releasing materials have a short-term efficiency, typically no longer than 24 h, which make them less suitable for longer applications (von Eiff et al. 2005). Moreover, most of these materials exhibit discontinuous release rate with an initially high release followed by an exponential decrease, that favours the development of anti-microbial resistance (Gharbi et al. 2012). Finally, coating materials often undergo to chemical damages with a loss of efficiency (Ghosh et al. 2012; Pechook et al. 2015; Sobieh et al. 2016).

Recently, the natural compounds zosteric acid (ZA) or *p*-(sulfoxy)cinnamic acid and salicylic acid (SA) have been proposed as alternative or integrative antimicrobial-free strategy to prevent biofilm development (Villa et al. 2010; Cattò et al. 2017). Instead of killing cells, ZA and SA influence the multicellular behaviour of microorganisms, ie microbial adhesion, cell-to-cell

communication signals and dispersion, massively decreasing biofilm development without imposing a selective pressure, thus limiting the drug-resistance development (Polo et al. 2014;). In previous studies of these authors, the structural requirements of ZA and SA necessary for biofilm inhibition as well as functional groups that could be exploited for their covalent linkage to an abiotic surface have been identified (Cattò et al. 2015; Cattò et al. 2017). These works revealed that the cinnamic acid moiety is responsible of the ZA anti-biofilm activity. Moreover, the introduction of an amino group in the *para* position of cinnamic acid moiety of ZA and on phenyl ring of SA does not affect their anti-biofilm activity and could be exploited for their covalent linkage to a polymeric support. Thanks to these information, the cinnamic acid active moiety of ZA and SA were subsequently covalently immobilized on a polyethylene surface by Dell'Orto et al. (2017) and oriented to externally exhibit their active scaffold. Since no molecules were leached from the surface, their concentration remained constantly effective and below the lethal level, reducing the risk of developing resistant strains. Although a detailed chemical work was previously performed, further development of this technology required a deeper microbiological investigation. In this work, the new bioengineered materials were investigated in-depth to assess their anti-biofilm performance, by using a laboratory model system to simulate conditions encountered in vivo. Moreover, the synergistic effect of these bio-hybrid materials coupled with traditional antimicrobial agents were investigated.

Materials and Methods

Polymeric surface preparation

Low density polyethylene (LDPE) coupons (round shape, d=1.27cm) were functionalized with ZA and SA derivatives according to Dell'Orto et al. (2017). Briefly, LDPE surface was activated

with a low pressure oxygen plasma treatment and graft-polymerized with 2-hydroxyethyl methacrylate (LDPE-OH). The terminal hydroxyl groups of HEMA side chains were converted into the carboxylic acid derivatives (LDPE-COOH) by treatment with succinic anhydride.

The cinnamic acid active moiety of ZA and SA have been modified by the insertion of an amino group in the *para* position of phenyl ring to give *p*-amino cinnamic acid and *p*-amino salicylic acid. Finally, a condensation reaction between the LDPE-COOH surface and the amino group was performed (LDPE-CA and LDPE-SA).

Escherichia coli *strain and growth condition*

E. coli strain MG1655 was used as a model system for bacterial biofilms, being a cosmopolitan bacterium that shares a core set of genes with clinically-relevant serotypes and foodborne pathogenic strains, including genes involved in biofilm formation (Faucher and Charette, 2015). The strain was stored at -80 °C in suspensions containing 20% glycerol and 2% peptone, and was routinely grown in Luria-Bertani broth (LB, Sigma-Aldrich) at 37 °C.

Biofilm growth in the CDC Reactor

E. coli biofilm was grown on non-functionalized (LDPE, LDPE-OH and LDPE-COOH) and functionalized (LDPE-CA and LDPE-SA) coupons in the Center for Disease Control biofilm reactor (CDC reactor, Biosurface Technologies, Bozeman, MT, USA) according to Cattò et al. (2017). Briefly, the bioreactor was inoculated with 400 ml of sterile LB medium with the addition of 1 ml of diluted pre-washed overnight culture containing 10^7 cells of *E. coli*. The culture was grown at 37°C with continuous stirring for 24 h. When the 24-h adhesion phase was over, the peristaltic pump was started and sterile 10% LB medium was continuously pumped into

the reactor at a rate of 8.3 ml min^{-1}. After 48 h of dynamic phase, functionalized and non-functionalized coupons were removed, gently washed with phosphate buffered saline (PBS, 0.01 M phosphate buffer, 0.0027 M potassium chloride pH 7.4) and processed to be analyzed.

Plate count viability assay

Collected coupons were transferred to 5 ml of PBS and sessile cells were removed from the coupon surface by 30 s vortex mixing and 2 min sonication (Branson 3510, Branson Ultrasonic Corporation, Dunburry, CT) followed by other 30 s vortex mixing. Serial dilutions of the resulting cell suspensions were plated on Tryptic Soy Agar (TSA, Fisher Scientific) and incubated overnight at 37 °C. Colony forming units (CFUs) were determined by the standard colony counting method. Obtained data were reported as number of viable bacterial cells normalized to the area and means were calculated. The efficacy of the anti-biofilm material was calculated as percentage reduction of the CFUs in respect to the LDPE control. Four coupons for each surface were analyzed. The experiment was repeated four times for a total of 16 coupons analyzed.

Epifluorescence microscopy analysis

The percentage of live and dead cells in the biofilm biomass grown on both non-functionalized and functionalized coupons was determined using the Live/Dead BacLight viability kit (L7012, Molecular Probes-Life Technologies). Biofilm was incubated with 2 µl of each fluorescent probe per ml of sterile filtered PBS at room temperature in the dark for 25 min and then rinsed with sterile PBS, according to the manufacturer's instruction. Coupons without biofilm were also stained with the dyes in order to exclude any false positive signals. Biofilm samples were

visualized using a Nikon Eclipse E800 epifluorescent microscope with excitation at 480 nm and emission at 516 nm for the green channel and excitation at 581 nm and emission at 644 nm for the red channel. Images were captured with a 60x, 1.0 NA water immersion objective and analyzed via MetaMorph 7.5 software (Molecular Devices, Sunnyvale, CA, USA). The percent area of stained cells was obtained by calculating at least ten random images for each sample. The efficacy of the anti-biofilm material was calculated as percentage reduction in stained cells area in respect to the LDPE control images. Relative viability within the biofilm was determined by dividing the percent area of the alive cells by the percent area of the dead cells in each sample. Four coupons of each surface were analyzed in each experiment. The experiment was repeated four times for a total of 16 coupons analyzed.

Confocal Laser Scanning Microscopy (CLSM) analysis

Three-D morphology of biofilm growth on non-functionalized and functionalized surfaces was analyzed by CLSM. Biofilm was stained with 200 μg ml^{-1} lectin Concanavalin A-Texas Red conjugate dye (C825, Molecular Probes-Life Technologies) to visualize the polysaccharide component of the extracellular polymeric substances (EPS) and 1:1000 Sybr green I fluorescent nucleic acid dye (S7563, Molecular Probes-Life Technologies) to display biofilm cells, in the dark for 30 min. Coupons without biofilm were also stained in order to exclude any false positive signals. Biofilm samples were visualized using a Leica SP5 CLSM with excitation at 488 nm, and emission <530 nm (green channel). Images were captured with a 63x, 0.9 NA water immersion objective and projections and 3D-reconstructed images of biofilm were generated using the Imaris software package (Bitplane Scientific Software, Zurich, Switzerland).

Quantitative biofilm structural parameters were calculated, including (i) mean thickness, which identifies the mean distance from the substrate in the direction normal to the substrate where there is biofilm; (ii) roughness, a quantity calculated from the thickness distribution and that describes the heterogeneity of the biofilm; (iii) substratum coverage, the percentage of substrate area occupied by the biofilm; (iv) surface-to-volume ratio, which reflects the fraction of biofilm area that is exposed to the nutrients; and (v) bio-volume, of both cells polysaccharide matrix, which provides an estimation of the biomass in the biofilm (Chang et al. 2015). Biofilm morphological parameters were obtained via MetaMorph 7.5 (Molecular Devices, Sunnyvale, CA, USA) and COMSTAT software from at least five random images for each sample according to Heydorn et al. (2000). Four coupons of each surface were analyzed. The experiment was repeated four times for a total of 16 coupons analyzed.

Antimicrobial susceptibility test

Non-functionalized and functionalized coupons with pre-grown biofilm were removed from the CDC reactor and independently soaked in 15 ml of 100 μg ml^{-1} ampicillin (Amp, BP1760-5, Fisher Scientific) for 24 h and 20% ethanol for 20 min. Negative controls were set up by soaking coupons with pre-grown biofilm in 15 ml of PBS for 24 h or 20 min. The concentrations and the incubation time were chosen to mimic antibiotic therapies and daily disinfection procedures with ethanol in hospital and industrial settings. After the treatment, coupons were left in PBS for 10 min in order to neutralize the antimicrobial agent. Cells in the biofilm were dislodged from the coupon and collected in PBS for colony counting, as previously reported in the ‘plate count viability assay section’. Cells dispersed in the bulk liquid were washed by centrifugation at 8000 g for 30 min and suspended in PBS for colony counting. Efficacy of both ampicillin and ethanol

treatments was reported as percentage reduction in respect to the LDPE control treated with PBS. For each experiment, four coupons of each surface were analyzed. The experiment was repeated four times for a total of 16 coupons analyzed.

The antimicrobial activity of 20% ethanol on *E. coli* biofilm pre-grown on non-functionalized and functionalized coupons was further investigated by using a CLSM method that enables the direct and real-time visualization of cell inactivation within the biofilm structure (Davison et al. 2010). The imaging technique was based on monitoring the loss of fluorescence that corresponds to the leakage of a fluorophore out of cells due to the membrane permeabilization by the biocides (Davison et al. 2010). The experiment was carried out using the FC 270 flow cell apparatus (BioSurface Technologies, Bozeman, MT), according to the manufacturer's recommendations. Biofilms pre-grown on the coupons were stained with 5 mM of syto-9 green fluorescent nucleic acid stain solution (S-34854, Molecular Probes-Life Technologies) in PBS at room temperature in the dark for 30 min and then rinsed with PBS. A solution of 20% ethanol was pumped through the flow cells at a 1 ml min^{-1} rate for 20 min. The spatiotemporal decrease of fluorescence intensity was observed using a Leica SP5 CLSM with excitation at 488 nm, and emission <530 nm (green channel) and a 63x, 0.9 NA water immersion objective. Images were analyzed by Imaris (Bitplane Scientific Software, Zurich, Switzerland) according to Davison et al. (2010). The average green fluorescence intensity was measured at different locations within the biofilm: at the interface with the bulk fluid (top), the intermediate location (centre) and the interface with the coupon (bottom). Changes in intensity were normalized by the initial intensity at the beginning of the 20-min antimicrobial treatment. This normalized intensity was used to compare values of relative loss of fluorescence during 20-min biocide treatment periods. The kinetics of fluorescence loss was quantified by the parameter T_{50}, the time elapsed from the initiation of

treatment until the fluorescence intensity falls to half of its initial value at a particular spot. Three coupons of each surface were analyzed. The experiment was repeated three times for a total of 9 coupons analyzed.

Statistical Analysis

Two-tailed ANOVA analysis, via a software run in MATLAB environment (Version 7.0, The MathWorks Inc, Natick, USA), was applied to statistically evaluate any significant differences among the samples and concentrations. The ANOVA analysis was carried out after verifying data independence (Pearson's Chi-square test), normal distribution (D'Agostino-Pearson normality test) and homogeneity of variances (Bartlett's test). Tukey's honestly significant different test (HSD) was used for pairwise comparison to determine the significance of the data. Statistically significant results were depicted by p-values < 0.05.

Results

LDPE-CA and LDPE-SA reduce biofilm biomass without affecting cell viability

Experiments showed that LDPE-CA and LDPE-SA had an optimal anti-biofilm performance, reducing viable adhered cells by 61.6±10.5% and 60.0±10.6% respectively in comparison to the LDPE control surface (Table 1). No significant differences were detected in viable adhered cells among the LDPE control and the LDPE-OH and LDPE-COOH linker samples (Table 1).

Epifluorescence microscopic techniques were additionally used to provide image analysis and in-situ quantification of bacterial cells. Figure 1 shows direct microscope visualizations of the total biofilm biomass on functionalized and non-functionalized coupons and stained for live and dead cells. Microscope assay revealed that differences in dead cells data were not statistically relevant

(Table 1, Figure 1A). On the contrary, biofilms on LDPE-CA and LDPE-SA showed a significantly decrease in the number of live cells, corresponding to 56.7±11.4% and 70.6±7.3% in respect to the LDPE control sample (Table 1, Figure 1B-C), confirming results obtained in the plate count viability assay. No significant differences were detected in live cells data between the LDPE and the LDPE-OH and LDPE-COOH linker samples (Table 1).

Coupons without biofilm and stained with the same dye did not produce detectable fluorescence and therefore no false positive signals were produced.

LDPE-CA and LDPE-SA affect biofilm morphology

Projection analysis as well as 3D-reconstructed CLSM images showed a complex biofilm on LDPE, LDPE-OH, LDPE-COOH, with an intense red and green signal corresponding to multi-layers of cells organized in macro-colonies inside a well-structured polysaccharide matrix (Figure 2A-B). On the contrary, biofilm growth on LDPE-CA and LDPE-SA resulted in a significant decrease of thickness with a mono-layer of dispersed cells (green signal) and very low presence of polysaccharide matrix (red signal) (Figure 2C-F). Coupons without biofilm and stained with the same dye did not produce detectable fluorescence therefore false positive signals were not produced.

Biofilms on both the functionalized surfaces displayed a thickness below 5 μm with a decrease up to 84.5±1.2% (Table 2). On the contrary, biofilm on LDPE control surface reached about 25 μm thick. Additionally, the LDPE-CA and LDPE-SA biofilm roughness resulted significantly decreased (up to 57.0±3.9%) indicating a uniform biofilm layer in contrast with the patchy and more heterogeneous control biofilm. On LDPE-CA and LPDE-SA, the substratum coverages by biofilm were notably lower (up to 84.5±2.5%) than in the corresponding non-functionalized

counterpart as well as the total bio-volumes (up to 92.0±6.5%). Indeed, LDPE-CA and LDPE-SA reduced cellular (by 91.2±14.1% and 90.1±13.7% respectively) and polysaccharide matrix bio-volumes (by 99.9±11.3% and 94.0±16.7% respectively), in comparison to the LDPE control surface. The matrix/cells bio-volumes ratio displayed value over 1 in biofilm grown on LDPE, meaning a predominance of matrix in respect to the cells. A significant reduction of matrix/cells ratio was found within the biofilm grown on LDPE-CA and LDPE-SA, with value equal (LDPE-SA) or under 1 (LDPE-CA), confirming a relevant decrease in the matrix amount. As a consequence, the biofilm exposed surface/bio-volume ratio significantly increased when biofilm was grown on LDPE-CA (16.8±0.4 fold) and LDPE-SA (7.1±0.2 fold). No significant differences were detected in all morphological parameters between biofilms grown on LDPE, LDPE-OH and LDPE-COOH materials.

LDPE-CA and LDPE-SA enhance biofilm susceptibility toward antimicrobial agent

To evaluate the synergistic effect of functionalized materials with traditional antimicrobial agents, biofilm pre-grown on LDPE control surface and LDPE-CA and LDPE-SA was independently submitted to a treatment with 100 μg ml^{-1} ampicillin and 20% ethanol.

The 24 h treatment with ampicillin did not significantly affect the number of viable cells in the biofilm pre-grown of LDPE surface in comparison to the biofilm grown on the same surface but treated with PBS (Table 3). On the contrary, the combination of both LDPE-CA and LDPE-SA with ampicillin reduced biofilm biomass by 96.1±15.4% and 95.5±16.9%, respectively, in comparison to the LDPE surface treated with PBS. Indeed, the treatment with ampicillin further decreased the number of viable cells by 37.2±6.3% and 32.0±4.9% respectively on LDPE-CA and LDPE-SA than the functionalized surfaces alone did. In the bulk liquid, no statistical

differences were detected among the number of live cells from any surface after the ampicillin treatment. Interestingly, PBS alone weakly increased the number of cells dispersed from LDPE-CA and LDPE-SA biofilms.

The 20-min treatment with 20% ethanol did not significantly affect the number of viable cells in the biofilm grown on the LDPE surface (Table 3). In contrast, the combination of both LDPE-CA and LDPE-SA with ethanol reduced biofilm biomass by 89.2±12.3% and 86.5±8.9%, respectively, in comparison to the LDPE control surface treated with PBS. Indeed, the treatment with ethanol further decreased the number of viable cells by 20.3±2.5% and 27.8±2.5% on LDPE-CA and LDPE-SA, respectively, than the functionalized surface alone did. No statistical differences were detected among the number of live cells from any surface after the ethanol treatment in the bulk liquid.

The direct time-lapse CLSM analysis of the 20% ethanol effect on a biofilm pre-grown on both LDPE control and LDPE-CA and LDPE-SA functionalized surfaces was additionally performed. The penetration of ethanol was inferred from the loss of green fluorescence in the biofilm during the treatment. The time-lapse images showed that ethanol treatment did not affect green fluorescence of biofilm grown on the LDPE control within the 20 min of the experiment (Figure 3A). Moreover, no spatiotemporal changes were detected (Figure 3B-C). On the contrary, the ethanol treatment on biofilm grown on both LDPE-CA and LDPE-SA significantly affected the biofilm biomass integrity, leading to a rapid and complete loss in fluorescent intensity (Figure 3A). The highest T_{50} resulted at the bottom of the biofilm, at the contact with the coupon surface, and the lowest at the biofilm surface, at the interface with the bulk liquid. Indeed, on LDPE-CA, T_{50} values were found 10.8±1.5-fold and 1.2±0.03-fold higher, respectively, at the bottom and in the center of the biofilm in respect to the top (Figure 3B-C). Also in the biofilm on LDPE-SA,

T_{50} progressively decreased from the bottom to the centre, with values respectively 40.0±1.2-fold and 4.5±0.3-fold higher in comparison to the top (Figure 3B-C). T_{50} at the bottom was 3.8±0.06-fold higher in the biofilm grown on LDPE-CA in comparison to that grown on LDPE-SA, while no differences in the T_{50} were detected at the centre and the top of the biofilm (Figure 3C).

Discussion

In this work, the functionalization of LDPE surface with biocide-free anti-biofilm compounds, ie ZA and SA, was carried out to obtain new no-toxic materials able to hinder biofilm formation. LDPE has been chosen as the most commonly widespread polymer in many applications, eg biomedical devices (Siddiqua et al. 2015) and food packaging (Raj et al. 2004), due to its excellent chemical resistance, low wetting properties in aqueous media, high impact strength, light weight and high flexibility (Sastri 2010). Notably, up to now, the functionalization was performed only when polymeric material is a film, with

thickness around few nanometres. In this work 1.6 mm thickness LDPE coupons were used opening the perspective to extend the technology to other materials with similar thickness.

In a first step of the research ZA and SA have been modified to be suitable for their covalent grafting to the LDPE surface.

In a previous work the authors demonstrated that the cinnamic scaffold is the specific structural feature responsible for the ZA anti-biofilm performance (Cattò et al. 2015). Moreover structure-anti-biofilm activity relationship studies revealed that the anti-biofilm activity of ZA and its derivatives depended upon the presence of a carboxylate anion and, consequently, on its hydrogen-donating ability. In addition, the conjugated aromatic system was instrumental to the anti-biofilm activities of ZA since the presence of the double bond stabilized the carboxylate

anion. In contrast, the sulfate group is not instrumental for the ZA anti-biofilm activity and its presence in ZA structure is part of an ecological phytostrategy to make the active cinnamic moiety more soluble and thus more mobile in the water-based sap of the vascular transport system (Baek et al. 2010). In line with the previous research, in this work ZA has been modified by replacing the sulphate group in the para position of the phenyl ring with an amino group suitable for a condensation reaction with the LDPE-COOH surface. Cattò et al. (2015) identified *p*-amino cinnamic acid as an excellent candidate to be covalently linked to a polymeric support. Moreover, *p*-aminocinnamic displayed anti-biofilm activity, suggesting that the addition of an amino group in the *para* position of phenyl ring of cinnamic acid moiety does not affect the anti-biofilm performance of the molecule. Similarly, Cattò et al. (2017) demonstrated that the addition of the amino group in the *para* position of SA phenyl ring does not affect its anti-biofilm performance. Moreover, docking calculations suggested that the presence of the amino group only slightly influences the binding mode to the tryptophanase TnaA targeted protein predicted for SA, with a mechanism of action that involves the same protein residues expected for SA. Thus, an amino group in the *para* position of phenyl ring has been added to the SA chemical structure, allowing its covalent binding with the LDPE-COOH surface.

In the past, ZA and SA were already incorporated in different polymeric materials able to gradually release the anti-biofilm molecules in the surrounding area (Geiger et al. 2004; Barrios et al. 2005; Rosenberg et al. 2008; Nowatsky et al. 2012). However, in most cases these systems showed several problems such as the non-uniform distribution of the anti-biofilm compounds inside the material and the formation of aggregates due to the incomplete miscibility of the molecules in the polymers. In addition, a constant release rate of the active compound has neither been achieved nor monitored, limiting the effectiveness of the technology to only a short period

of time and making this system often unfeasible for a wide range of practical applications (Barrios et al. 2005; Nowatsky et al. 2012). Here, all these issues have been addressed as ZA and SA are uniformly distributed and oriented to externally exhibit their active scaffold. This allows the functionalized material to directly interact with bacterial cells even at the early stages of biofilm formation (Dell'Orto et al. 2017). In this work, the efficacy of the anti-biofilm materials was evaluated in depth with the perspective to transfer the technology into consumer products suitable for a widespread distribution.

A laboratory standard procedure using a CDC biofilm reactor was employed to grow *E. coli* biofilms simulating conditions to which surfaces of a wide range of applications are subjected during their use (Goeres et al. 2005; Gilmore et al. 2010; Williams et al. 2011). Experiments revealed that biofilms were significantly affected when grown on both LDPE-CA and LDPE-SA in comparison to the LDPE surface. Indeed, according to the anti-biofilm ranges proposed by Cattò et al. (2015), LDPE-CA and LDPE-SA displayed optimal anti-biofilm performance decreasing viable biomass over the 60% in comparison to the control material. Moreover, in-situ stained biofilm for live and dead bacterial cells confirmed that the reduction in the biofilm biomass was achieved in both functionalized surfaces by a mechanism that did not affect bacterial viability, an important factor in the challenge to limit the risk of developing resistant microbial strains. Results are in line with those previously achieved with ZA and SA free in solution. Villa et al. (2010) found that 500 mg l^{-1} ZA reduced *E. coli* cells adhesion up to 70% whereas Cattò et al. (2017) proved that 25 mg l^{-1} SA inhibited *E. coli* biofilm by the 68%. In both cases the anti-biofilm performances were displayed with a mechanism more subtle than simple killing activity, modulating the activity of some ZA and SA targeted proteins and providing

conditions to which the best microbial strategy is to escape from the adverse conditions, instead of persisting in a biofilm lifestyle.

Additional experiments performed by CLSM showed the massive impacts of the functionalized material on biofilm morphology. Biofilm grown on LDPE-CA and LDPE-SA showed a significant decrease in thickness and roughness with a uniform mono-layer of dispersed cells and a significant lower bio-volume of polysaccharide matrix. On the contrary, LDPE control images showed a complex heterogeneous biofilm, with an intense fluorescence signal corresponding to dense multi-layers of cells uniformly distributed over the substratum and organized in macro-colonies inside a well-structured robust polysaccharide matrix. Cattò et al. (2017) showed that SA free in solution significantly decreased the amount of polysaccharide in the matrix of *E. coli* biofilm while Vila and Soto (2012) hypothesised that SA plays a role in the matrix production decreasing the expression of the membrane protein, OmpA, involved in the transport of polymeric substances required for the formation of the EPS outside the cells.

The exposed biofilm surface to bio-volume ratio, which reflects the fraction of biofilm area that is exposed to the nutrient flow, was higher in the biofilm grown on the functionalized surfaces with respect to the biofilm grown on the non-functionalized counterpart. High surface to bio-volume ratio indicated the presence of small cell clusters attached to the substratum while low value indicated the occurrence of larger micro-colonies within the biofilm (Mangwani et al. 2016). Indeed, surface to bio-volume ratio is an indicative parameter of adaptation of the biofilm to the environment and it is reported to increase in stress conditions (Heydorn et al. 2000; Bester et al. 2011; Mangwani et al. 2016).

Experiments showed no significant differences in adhered cells, cell viability and biofilm quantitative structural parameters between the LDPE control surface and the LDPE-OH and

LDPE-COOH linker surfaces. These results suggested that functionalization procedure did not introduce modification in LDPE structure that affected cell adhesion and viability as well as biofilm morphology. Consequently, the anti-biofilm performance of LDPE-CA and LDPE-SA was totally attributable to ZA and SA covalently immobilized on the surface. Indeed, data suggested that ZA and SA functionalized on a LDPE surface are able to exert their anti-biofilm activity even immobilized on a surface, providing data comparable with those previously reported with the same molecules free in solution.

The combination of anti-biofilm surfaces with conventional treatments could be a step forward to maximize the anti-biofilm performance of the polymeric materials. Surfaces that retard adhesion and consequently biofilm formation greatly enhance the efficiency of cleaning treatments and disinfection procedures, because, once biofilm integrity is affected, bacteria are more susceptible to conventional antimicrobial agents than those in the intact biofilms, allowing to reduce the antimicrobial doses and providing more potent control against the development of drug-resistance strain (Cui et al. 2015; Cheeseman et al. 2017).

In this study, the ability of LDPE-CA and LDPE-SA to enhance biofilm sensitivity to conventional antimicrobial agents, ie ampicillin and ethanol, has been shown. Indeed, both ampicillin and ethanol significantly further decreased the number of viable adhered cells on both functionalized materials with respect the non-functionalized controls. CLSM analysis revealed that biofilms grown on LDPE-CA and LDPE-SA were deeply affected with an extremely low amount of polysaccharide matrix. The biofilm matrix is a barrier with the potential to reduce the penetration of antibiotics or biocides within the biofilm, either by physically slowing their diffusion or chemically reacting with them (Rabin et al. 2015). Although we do not exclude the involvement of other mechanisms, biofilm grown on functionalized materials might be more

susceptible to antimicrobial agents as these compounds can penetrate more easily within the biofilm matrix, exerting their effect even at a concentration below those normally used in the traditional applications.

Beside the interesting results, an integrative solution by coupling a functionalized material with ethanol could have wider applications than a strategy with ampicillin. Ethanol is the most popular broad range bactericidal agent (McDonnel and Russell, 1999). It is used in the disinfection of skin, medical apparata, cooking equipment etc. because it is volatile, leaves minimal residue, and is harmless, even if intraoral intake occurs. Despite its extensive and long-standing use as an antiseptic, there is no evidence of acquired microbial resistance (Balestrino et al. 2009). Importantly, ethanol is universally available without restriction and with an affordable price. On the contrary, antibiotic resistance is a global issue and sooner or later, after several antibiotic treatments, ampicillin resistance naturally occurs (Ventola, 2015). Moreover, antibiotic treatment is limited to only few sectors of the economy, ie medical sector, and their use often requires a prescription. On the basis of these considerations, the spatial and temporal patterns of ethanol penetration into the biofilm pre-grown on both non-functionalized and functionalized surfaces were additionally investigated by direct time-lapse CLSM analysis. This method is suitable for mimicking antimicrobial treatments that cause membrane permeabilization, eg ethanol (Davison et al. 2010; Corbin et al. 2011). The biofilm on LDPE surface retained its initial fluorescence over the 20-min experimental test, while ethanol caused a loss of fluorescence in the biofilms pre-grown on both LDPE-CA and LDPE-SA. A distinct spatiotemporal pattern of fluorescence loss was observed for both the surfaces investigated. In both cases the antimicrobial action of ethanol occurred very fast at the biofilm surface and slower at the bottom of biofilm, in contact with the coupon surface. However, at the bottom of

biofilm the decrease of fluorescence intensity resulted 3.8±0.06-fold more rapid in the biofilm grown on LDPE-SA in respect to that grown on LDPE-CA, suggesting a stronger action of ethanol against biofilm on LDPE-SA rather than on LDPE-CA. The direct time-lapse CLSM analysis did not give evidence if the treatment caused the killing or the removal of the biomass from the biofilm or both. The loss of green colour proved that cell membranes have been compromised, not killed (Corbin et al. 2011). In addition, the plate count assay of cells in the bulk liquid after ethanol treatment performed in the previous experiments suggested the presence of a number of live cells.

The low toxicity of both ZA and SA are promising for spreading this technology to different sectors of the economy resulting in new, safe and eco-friendly types of products suitable for applications not only in the more traditionally studied sector of the economy, ie medical area, but in other challenging fields, especially when the use of antimicrobial agents is limited for safety reasons, eg in the food industry. Indeed, a food packaging surface with immobilized anti-biofilm molecules would offer the advantage of extending the shelf life of food and preventing the growth of food-borne bacteria/pathogens at early stages without a direct addition of the preservative agents and in a way that only low level of preservative comes in contact with food. Additionally, industrial installation and pipelines, such as drinking water networks, could take benefit from this research, providing safe material for water distribution systems that, at the same time, maintains high purity standard levels of water and limits the need of the less effective and expensive disinfection procedures.

Moreover, in addition to *E. coli*, the technology might be potentially used with a broad-spectrum activity against mixed infections. Most of the proteins targeted by ZA and SA are highly conserved with often a 100% of identity in a number of microorganisms including pathogens that

are a concern in the food processing industry, health-care sector and that are responsible of extensive damages to crops in the agricultural field (eg *Pseudomonas* spp., *Klebsiella* ssp., *Salmonella* ssp., *Shigella* spp, *Candida* spp., *Fusarium* spp.) (Cattò et al. 2015; Cattò et al. 2017). Additionally, ZA free in solution showed benefit against *Bacillus cereus*, *P. putida*, *Aspergillus niger*, *Penicillium citrinum*, *Candida albicans*, *Colletotricum lindemuthianum* and *Magnaporthe grisea* (Stanley et al. 2002; Villa et al. 2010, Villa et al. 2011; Polo et al. 2014) while SA have shown activity toward *P. aeruginosa*, *Klebsiella pneumoniae*, *Staphylococcus epidermidis*, *P. syringae*, *Pectobacterium carotovorum* and *C. albicans* (Muller et al. 1998; Faber and Wolff 1993; Dong et al. 2012; Lagonenko et al. 2013; Cattò et al. 2017). Thus, it is likely that LDPE-CA and LDPE-SA could exert their anti-biofilm activity also against other microorganisms.

Conclusion

In this work the active moiety of the natural compounds ZA and SA have been successfully immobilized on a LDPE surface providing a new class of polymeric materials with extended shelf-life and anti-biofilm properties superior to the conventional biocide-based approaches in terms of addressing the problem of detrimental biofilms. Indeed, the development of materials that can resist or prevent bacterial adhesion in a non-leaching modality and with biocidal free features constitutes a promising and emerging approach to deal with material-associated biofilms and an important achievement toward the dramatic increase of antimicrobial resistance among pathogens. Moreover, the covalent grafting guarantees the material long life as the molecules become permanently attached and integrated into the scaffold structure of polymers.

The work described in this paper could be extended to other polymeric materials as well as natural molecules. Notability, the use of plasma technology in the grafting procedure makes each surface, included those that do not possess the required chemical features, suitable for covalent binding, without changing the material bulk.

Beside this pioneering work, much can be done. So far, a multitude of natural compounds have revealed promising anti-biofilm properties suitable for the development of improved effective eco-friendly anti-biofilm materials (Villa et al. 2013). However, the functional groups required by these molecules to exert their anti-biofilm activity and, as a consequence, the binding site needed for their surface immobilization are poorly known or, even, completely unknown.

Acknowledgements

This work was supported by the Fondazione Cariplo under Grant number 2011−0277.

References

Ahire JJ, Hattingh M, Neveling DP, Dicks LM. 2016. Copper-containing anti-biofilm nanofiber scaffolds as a wound dressing material. PLoS One. 11:e0152755.

Baek D, Pathange P, Chung J-S, Jiang J, Gao L, Oikawa A, Hirai MY, Saito K, Pare PW, Shi H. 2010. A stress-inducible sulphotransferase sulphonates salicylic acid and confers pathogen resistance in Arabidopsis. Plant Cell Environ. 33:1383–1392.

Balestrino D, Souweine B, Charbonnel N, Lautrette A, Aumeran C, Traoré O, Forestier C. 2009. Eradication of microorganisms embedded in biofilm by an ethanol-based catheter lock solution. Nephrol Dial Transplant. 24:3204–3209.

Barrios CA, Xu Q, Cutright T, Newby BM. 2005. Incorporating zosteric acid into silicone

coatings to achieve its slow release while reducing fresh water bacterial attachment. Colloids Surf B Biointerfaces. 41:83–93.

Bester E, Kroukamp O, Hausner M, Edwards EA, Wolfaardt GM. 2011. Biofilm form and function: carbon availability affects biofilm architecture, metabolic activity and planktonic cell yield. J Appl Microbiol. 110:387–398.

Cattò C, Dell'Orto S, Villa F, Villa S, Gelain A, Vitali A, Marzano V, Baroni S, Forlani F, Cappitelli F. 2015. Unravelling the structural and molecular basis responsible for the anti-biofilm activity of zosteric acid. PLoS One. 10:e0131519.

Cattò C, Grazioso G, Dell'Orto S, Gelain A, Villa S, Marzano V, Vitali A, Villa F, Cappitelli F, Forlani F. 2017. The response of *Escherichia coli* biofilm to salicylic acid. Biofouling. 33:235–251.

Chang YW, Fragkopoulos AA, Marquez SM, Kim HD, Angelini TE, Fernandez-Nieves A. 2015. Biofilm formation in geometries with different surface curvature and oxygen availability. New J Phys. 17:033017.

Chen M, Yu Q, Sun H. 2013. Novel strategies for the prevention and treatment of biofilm related infections. Int J Mol Sci. 14:18488–18501.

Cheesman MJ, Ilanko A, Blonk B, Cock IE. 2017. Developing new antimicrobial therapies: are synergistic combinations of plant extracts/compounds with conventional antibiotics the solution?. Pharmacogn Rev. 11:57–72.

Coenye T, De Prijck K, Nailis H, Nelis HJ. 2011. Prevention of *Candida albicans* biofilm formation. Open Mycol J. 5:9–20.

Corbin A, Pitts B, Parker A, Stewart PS. 2011. Antimicrobial penetration and efficacy in an in vitro oral biofilm model. Antimicrob Agents Chemother. 55:3338–3344.

Cui JH, Ren B, Tong YJ, Dai HQ, Zhang LX. 2015. Synergistic combinations of antifungals and anti-virulence agents to fight against *Candida albicans*. Virulence. 6:362−371.

Davison WM, Pitts B, Stewart PS. 2010. Spatial and temporal patterns of biocide action against *Staphylococcus epidermidis* biofilms. Antimicrob Agents Chemother. 54:2920–2927.

Dell'Orto S, Cattò C, Villa F, Forlani F, Vassallo E, Morra M, Cappitelli F, Villa S, Gelain A. 2017. Low density polyethylene functionalized with antibiofilm compounds inhibits *Escherichia coli* cell adhesion. J Biomed Mater Res A. 105:3251–3261.

Dong Y, Huang C, Park J, Wang G. 2012. Growth inhibitory levels of salicylic acid decrease *Pseudomonas aeruginosa* fliC flagellin gene expression. JEMI. 16:73–78.

Farber BF, Wolff AG. 1993. Salicylic acid prevents the adherence of bacteria and yeast to silastic catheters. J Biomed Mater Res. 27:599–602.

Faucher SP, Charette SJ. 2015. Bacterial pathogens in the non-clinical environment. Front Microbiol. 6:331.

Geiger T, Delavy P, Hany R, Schleuniger J, Zinn M. 2004. Encapsulated zosteric acid embedded in poly 3-hydroxyalkanoate coatings - Protection against biofouling. Polym Bull. 52:65–72.

Gharbi A, Humblot V, Turpin F, Pradier CM, Imbert C, Berjeaud JM. 2012. Elaboration of antibiofilm surfaces functionalized with antifungal-cyclodextrin inclusion complexes. FEMS Immunol Med Microbiol. 65:257–69.

Ghosh M, Manivannan J, Sinha S, Chakraborty A, Mallick SK, Bandyopadhyay M, Mukherjee A. 2012. In vitro and in vivo genotoxicity of silver nanoparticles. Mutat Res Genet Toxicol Environ Mutagen. 749:60–69.

Gilmore BF, Hamill TM, Jones DS, Gorman SP. 2010. Validation of the CDC biofilm reactor as a dynamic model for assessment of encrustation formation on urological device materials. J

Biomed Mater Res B Appl Biomater. 93:128–140.

Goeres DM, Loetterle LR, Hamilton MA, Murga R, Kirby DW, Donlan RM. 2005. Statistical assessment of a laboratory method for growing biofilms. Microbiology. 151:757–762.

Hall-Stoodley L, Costerton JW, Stoodley P. 2004. Bacterial biofilms: from the natural environment to infectious diseases. Nat Rev Microbiol. 2:95–108.

Heydorn A, Nielsen AT, Hentzer M, Sternberg C, Givskov M, Ersbøll BK, Molin S. 2000. Quantification of biofilm structures by the novel computer program COMSTAT. Microbiology. 146: 2395–2407.

Lagonenko L, Lagonenko A, Evtushenkov A. 2013. Impact of salicylic acid on biofilm formation by plant pathogenic bacteria. J Biol Earth Sci. 3:B176–B181.

Lo J, Lange D, Chew BH. 2014. Ureteral stents and Foley catheters-associated urinary tract infections: the role of coatings and materials in infection prevention. Antibiotics. 3:87–97.

Mangwani N, Shukla SK, Kumari S, Das S, Rao TS. 2016. Effect of biofilm parameters and extracellular polymeric substance composition on polycyclic aromatic hydrocarbon degradation. Rsc Adv. 6:S7540–S7551.

McDonnell G, Russell AD. 1999. Antiseptics and disinfectants: activity, action, and resistance. Clin Microbiol Rev. 12:147–179.

Muller E, Al-Attar J, Wolff AG, Farber BF. 1998. Mechanism of salicylate-mediated inhibition of biofilm in *Staphylococcus epidermidis*. J Infect Dis. 177:501–503.

Nowatzki PJ, Koepsel RR, Stoodley P, Min K, Harper A, Murata H, Donfack J, Hortelano ER, Ehrlich GD, Russell AJ. 2012. Salicylic acid-releasing polyurethane acrylate polymers as anti-biofilm urological catheter coatings. Acta Biomater. 8:1869–1880.

Pechook S, Sudakov K, Polishchuk I, Ostrov I, Zakin V, Pokroy B, Shemesh M. 2015.

Bioinspired passive anti-biofouling surfaces preventing biofilm formation. J Mat Chem B. 3:1371–1378.

Polo A, Foladori P, Ponti B, Bettinetti R, Gambino M, Villa F, Cappitelli F. 2014. Evaluation of zosteric acid for mitigating biofilm formation of *Pseudomonas putida* isolated from a membrane bioreactor system. Int J Mol Sci. 15:9497–518.

Rabin N, Zheng Y, Opoku-Temeng C, Du Y, Bonsu E, Sintim HO. 2015. Biofilm formation mechanisms and targets for developing antibiofilm agents. Future Med Chem. 7:493–512.

Raj B, Udaya Sankar K, Siddaramaiah. 2004. Low density polyethylene/starch blend films for food packaging applications. Adv Polym Technol. 23:32–45.

Rosenberg LE, Carbone AL, Romling U, Uhrich KE, Chikindas ML. 2008. Salicylic acid-based poly(anhydride esters) for control of biofilm formation in *Salmonella enterica* serovar Typhimurium. Lett Appl Microbiol. 46:593–599.

Sastri VR. 2010. Commodity thermoplastics: polyvinyl chloride, polyolefin, and polystyrene. In: Sastri VR, editor. Plastics in medical devices: properties, requirements, and applications. Amsterdam (NL): Elsevier Inc; p. 73–119.

Siddiqa AJ, Chaudhury K, Adhikari B. 2015. Hydrophilic low density polyethylene (LDPE) films for cell adhesion and proliferation. RRJOM. 1:43–54.

Simões M, Simões LC, Vieira MJ. 2010. A review of current and emergent biofilm control strategies. LWT - Food Sci Technol. 43:573–583.

Sobieh SS, Kheiralla ZMH, Rushdy AA, Yakob NAN. 2016. In vitro and in vivo genotoxicity and molecular response of silver nanoparticles on different biological model systems. Caryologia. 69:147–161.

Sousa ACA, Pastorinho MR, Takahashi S, Tanabe S. 2014. History on organotin compounds,

from snails to humans. Environ Chem Lett. 12:117–137.

Stanley MS, Callow ME, Perry R, Alberte RS, Smith R, Callow JA. 2002. Inhibition of fungal spore adhesion by zosteric acid as the basis for a novel, nontoxic crop protection technology. Phytopathology. 92:378–383.

Ventola CL. 2015. The antibiotic resistance crisis: part 1: causes and threats. P&T 40:277–283.

Vila J, Soto SM. 2012. Salicylate increases the expression of marA and reduces in vitro biofilm formation in uropathogenic *Escherichia coli* by decreasing type 1 fimbriae expression. Virulence. 3:280–285.

Villa F, Albanese D, Giussani B, Stewart PS, Daffonchio D, Cappitelli F. 2010. Hindering biofilm formation with zosteric acid. Biofouling. 26:739–752.

Villa F, Pitts B, Stewart PS, Giussani B, Roncoroni S, Albanese D, Giordano C, Tunesi M, Cappitelli F. 2011. Efficacy of zosteric acid sodium salt on the yeast biofilm model *Candida albicans*. Microb Ecol. 62:584–598.

Villa F, Villa S, Gelain A, Cappitelli F. 2013. Sub-lethal activity of small molecules from natural sources and their synthetic derivatives against biofilm forming nosocomial pathogens. Curr Top Med Chem. 13:3184–204.

von Eiff C, Jansen B, Kohnen W, Becker K. 2005. Infections associated with medical devices: pathogenesis, management and prophylaxis. Drugs. 65:179–214.

Williams DL, Woodbury KL, Haymond BS, Parker AE, Bloebaum RD. 2011. A modified CDC biofilm reactor to produce mature biofilms on the surface of peek membranes for an in vivo animal model application. Curr Microbiol. 62:1657–1663.

Tables

	Plate count assay	Epifluorescence microscope analysis		
Surface	**Viable adhered cells (CFU cm^{-2})**	**Live cells (%)**	**Dead cells (%)**	**Relative viability**
LDPE	$(1.05\pm0.15) \times 10^{7\,a}$	$59.82\pm4.86^{\,a}$	$6.51\pm0.81^{\,a}$	$8.48\pm0.34^{\,a}$
LDPE-OH	$(1.05\pm0.10) \times 10^{7\,a}$	$55.79\pm4.24^{\,a}$	$7.05\pm0.42^{\,a}$	$7.84\pm0.75^{\,a}$
LDPE-COOH	$(1.03\pm0.17) \times 10^{7\,a}$	$59.19\pm2.19^{\,a}$	$7.07\pm0.44^{\,a}$	$7.37\pm1.24^{\,a}$
LDPE-CA	$(0.42\pm0.08) \times 10^{7\,b}$	$25.91\pm4.75^{\,b}$	$5.98\pm1.21^{\,a}$	$4.77\pm1.22^{\,b}$
LDPE-SA	$(0.40\pm0.07) \times 10^{7\,b}$	$17.61\pm3.34^{\,b}$	$6.81\pm0.70^{\,a}$	$2.68\pm0.62^{\,c}$

Table 1. Biomass within the biofilm grown on non-functionalized (LDPE, LDPE-OH, LDPE-COOH) and functionalized polyethylene surfaces (LDPE-CA, LDPE-SA) by plate count viability assay and epifluorescence analysis. Data represent the mean ± standard deviation of four independent measurements. Different superscript letters indicate significant differences (Tukey's HSD, $p \leq 0.05$) between the means of different surfaces.

	LDPE	LDPE-OH	LDPE-COOH	LDPE-CA	LDPE-SA
Thickness (μm)	25.36±7.06 [a]	20.4±4.43 [a]	23.91±7.13 [a]	3.82±1.11 [b] (-84.5±1.2)	5.00±1.00 [b] (-80.2±1.7)
Roughness	0.37±0.02 [a]	0.36±0.02 [a]	0.35±0.05 [a]	0.18±0.03 [b] (-51.8±10.5)	0.16±0.01 [b] (-57.0±3.9)
Substratum coverage (%)	68.40±5.02 [a]	64.44±2.49 [a]	62.19±1.42 [a]	14.37±3.83 [b] (-78.9±5.6)	10.62±1.72 [b] (-84.5±2.5)
Surface/bio-volume ($\mu m^2\ \mu m^{-3}$) × 10^{-1}	0.18±0.05 [a]	0.16±0.02 [a]	0.16±0.01 [a]	3.08±0.10 [b] (+16.8±0.4 fold)	1.65±0.69 [c] (+7.1±0.2 fold)
Total bio-volume ($\mu m^3\ \mu m^{-2}$)	91.03±12.25 [a]	92.51±11.66 [a]	90.62±9.20 [a]	3.85±0.09 [b] (-92.0±6.5)	9.18±0.21 [b] (-91.3±2.6)
Cells bio-volume ($\mu m^3\ \mu m^{-2}$)	34.46±7.48 [a]	35.59±3.64 [a]	32.48±4.44 [a]	3.85±0.09 [b] (-91.2±14.1)	4.48±0.35 [b] (-90.1±13.7)
Polysaccharide matrix bio-volume ($\mu m^3\ \mu m^{-2}$)	59.88±10.97 [a]	56.91±8.02 [a]	58.15±4.75 [a]	0.00±0.01 [b] (-99.9±11.3)	3.99±1.05 [b] (-94.0±16.7)
Matrix/cells bio-volume ratio	1.44±0.23 [a]	1.60±0.06 [a]	1.63±0.13 [a]	0.00±0.00 [b] (-88.4±3.0)	1.00±0.13 [c] (-99.9±0.1)

Table 2. Biofilm morphological parameters of biofilm grown on non-functionalized (LDPE, LDPE-OH, LDPE-COOH) and functionalized polyethylene surfaces (LDPE-CA, LDPE-SA). In the brackets, percentage reduction/increase in comparison to the LDPE control sample is reported. Data represent the mean ± standard deviation of four independent measurements. Different superscript letters indicate significant differences (Tukey's HSD, $p \leq 0.05$) between the means of different surfaces.

	Ampicillin (24 h)			
	Coupon		**Bulk liquid**	
	PBS	Amp	PBS	Amp
LDPE	$(1.13\pm0.18) \times 10^{7\ a}$	$(9.28\pm3.51) \times 10^{6\ a}$	$(3.39\pm0.35) \times 10^{7\ a}$	$(3.57\pm0.92) \times 10^{6\ c}$
LDPE-CA	$(4.05\pm1.07) \times 10^{6\ b}$	$(4.40\pm0.70) \times 10^{5\ c}$	$(4.13\pm0.46) \times 10^{7\ b}$	$(4.69\pm0.28) \times 10^{6\ c}$
LDPE-SA	$(4.72\pm0.52) \times 10^{6\ b}$	$(5.12\pm0.91) \times 10^{5\ c}$	$(4.16\pm0.29) \times 10^{7\ b}$	$(3.84\pm0.38) \times 10^{6\ c}$
	Ethanol (20 min)			
	Coupon		**Bulk liquid**	
	PBS	EtOH	PBS	EtOH
LDPE	$(1.07\pm0.13) \times 10^{7\ a}$	$(1.00\pm0.04) \times 10^{7\ a}$	$(3.39\pm0.34) \times 10^{7\ a}$	$(1.87\pm0.08) \times 10^{6\ b}$
LDPE-CA	$(3.32\pm0.32) \times 10^{6\ b}$	$(1.16\pm0.16) \times 10^{6\ c}$	$(4.13\pm0.60) \times 10^{7\ a}$	$(5.39\pm0.50) \times 10^{6\ b}$
LDPE-SA	$(4.41\pm0.78) \times 10^{6\ b}$	$(1.44\pm0.15) \times 10^{6\ c}$	$(4.16\pm0.51) \times 10^{7\ a}$	$(9.53\pm0.17) \times 10^{6\ b}$

Table 3. Viable adhered cells (CFU cm^{-2}) on non-functionalized (LDPE) and functionalized coupons (LDPE-CA, LDPE-SA) and those released in the surrounding bulk liquid after a 24 h treatment with 100 µg ml^{-1} ampicillin or PBS and a 20 min treatment with 20% ethanol or PBS. Data represent the mean ± standard deviation of four independent measurements. Different superscript letters indicate significant differences (Tukey's HSD, $p \leq 0.05$) between the means of different surfaces and treatment.

Figures

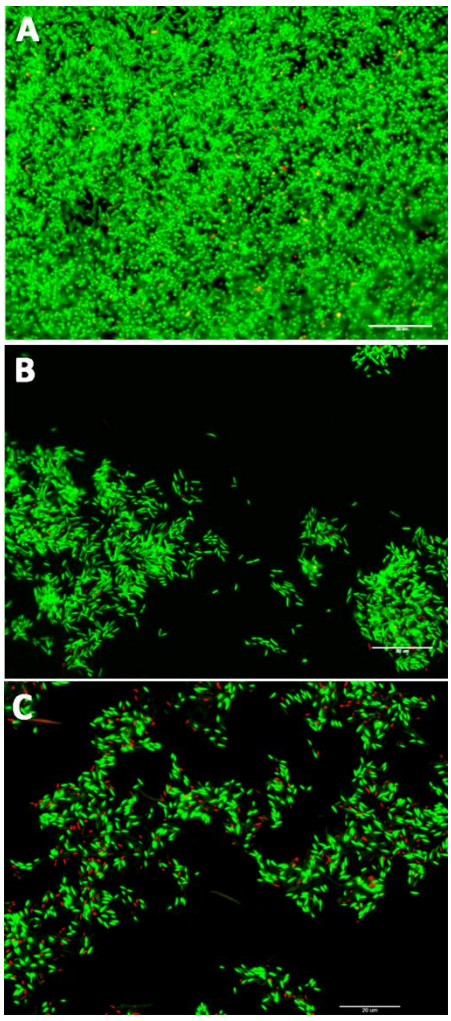

Figure 1. Epifluorescence microscope analysis. Representative epifluorescence microscope images of *E. coli* biofilm stained with Live/Dead BacLight viability kit and grown on non-functionalized LDPE, LDPE-OH, LDPE-COOH surfaces (A) and LDPE-CA (B) and LDPE-SA (C) functionalized surfaces (60x, 1.0 NA water immersion objective). Green fluorescence corresponds to *E. coli* live cells (λ_{ex}: 480 nm and λ_{em}: 516 nm) and red fluorescence corresponds to *E. coli* dead cells (λ_{ex}: 581 nm and λ_{em}: 644 nm). Scale bar = 20 µm.

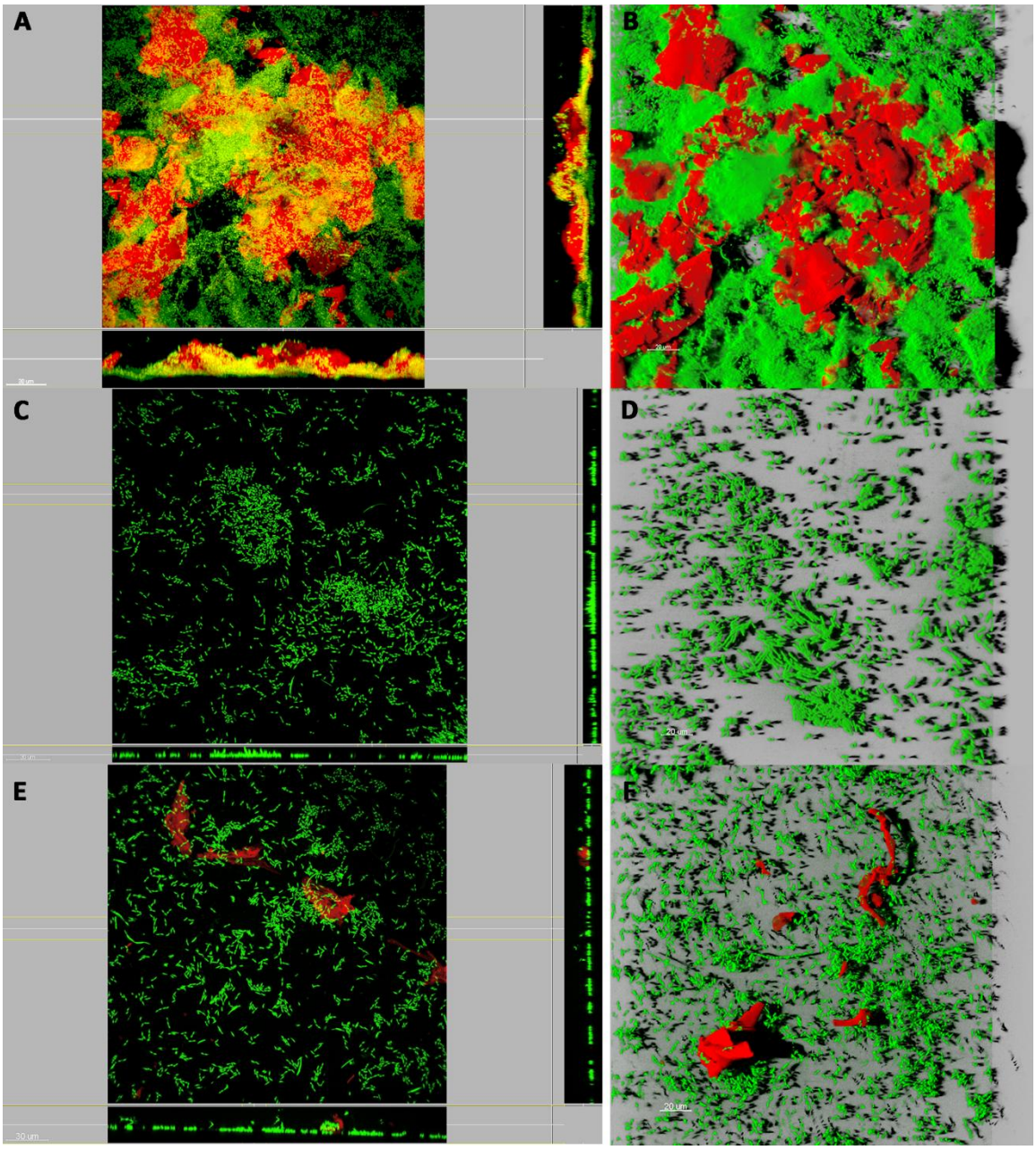

Figure 2. Confocal laser scanning microscopy analysis. Representative projection analysis (column on the left) and 3D-reconstructed CLSM images (column on the right) of *E. coli* biofilm grown on non-functionalized LDPE, LDPE-OH, LDPE-COOH surfaces (A, B) and LDPE-CA (C, D) and LDPE-SA (E, F) functionalized surfaces (λ_{ex} at 488 nm, and λ_{em} <530 nm, 60x, 0.9 NA water immersion objective). Live cells were stained green with Syber green I, whereas the polysaccharide matrix was stained red with Texas Red-labelled ConA. Scale bar= 20 or 30 µm.

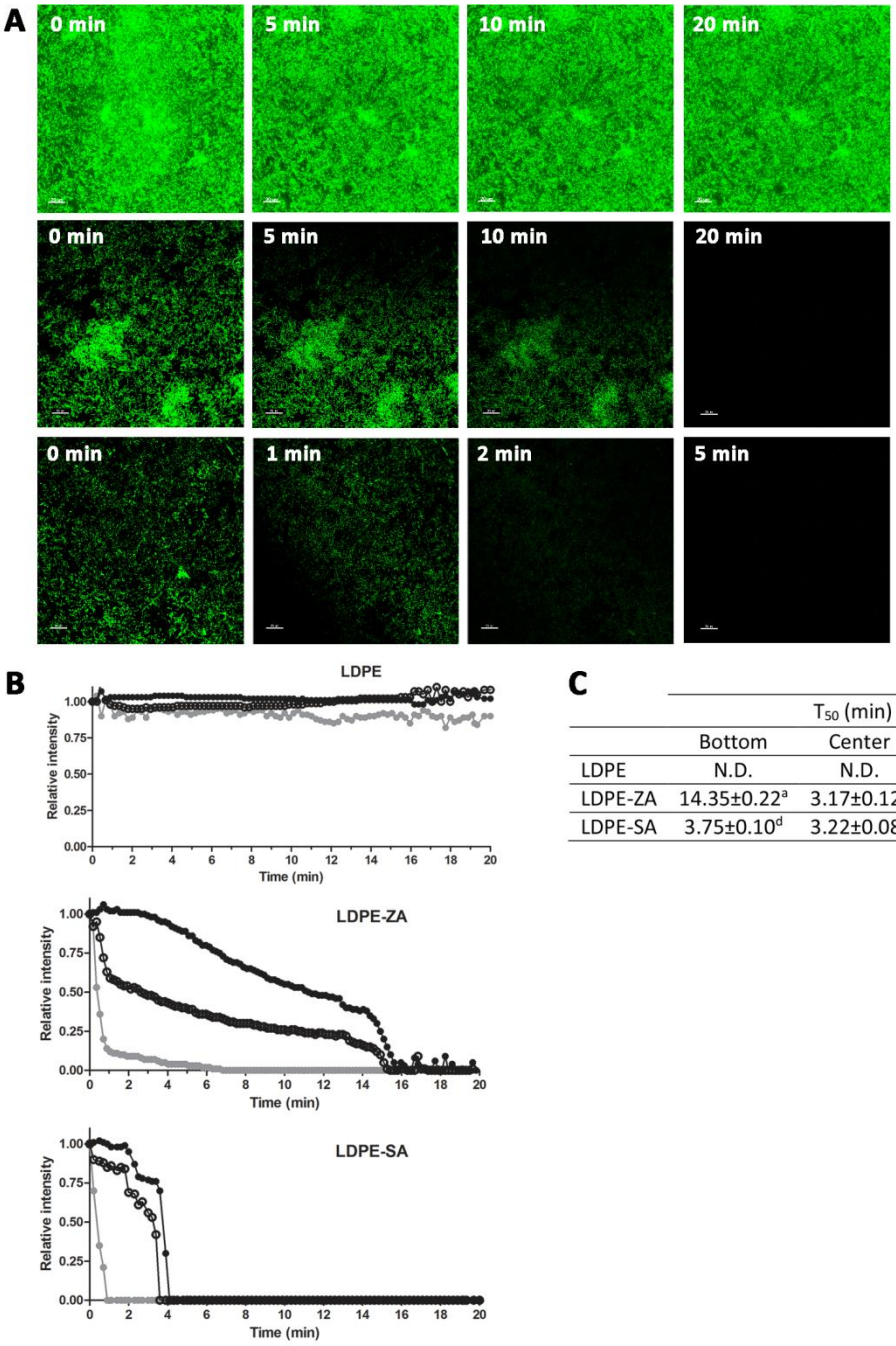

C

	T_{50} (min)		
	Bottom	Center	Top
LDPE	N.D.	N.D.	N.D.
LDPE-ZA	14.35±0.22^{a}	3.17±0.12^{b}	0.36±0.05^{c}
LDPE-SA	3.75±0.10^{d}	3.22±0.08^{b}	0.35±0.05^{c}

Figure 3. Antimicrobial susceptibility test. Time-lapse CLSM analysis of the 20% ethanol action against *E. coli* biofilm pre-grown on non-functionalized and functionalized polyethylene surfaces within the 20 min experimental test. A: Time-lapse CLSM representative images of biofilm pre-grown on LDPE control surface (first line), LDPE-CA (second line) and LDPE-SA (third line) during the treatment with 20% ethanol. Live cells were stained green with Syto 9 (λ_{ex}

at 488 nm, and λ_{em} <530 nm, 60x, 1.0 NA water immersion objective). Scale bar = 20 µm. B: Relative fluorescence intensity against the time at the interface with the bulk fluid (gray symbols), at the intermediate location (open symbols) and at the interface with the coupon (black symbols). Fluorescent intensity in a specific biofilm region was normalized by the initial intensity in that same region. C: The T_{50} parameter (time elapsed from the initiation of treatment until the fluorescence intensity fell to half of its initial value at a particular spot) calculated at the interface with the bulk fluid (top), at the intermediate location (center) and at the interface with the coupon (bottom). ND, not determined as fluorescence intensity did not reach 50% of initial intensity within the experimental time.